Hindawi
International Journal of Energy Research
Volume 2023, Article ID 7880842, 18 pages
https://doi.org/10.1155/2023/7880842

Research Article

Design and Operation Optimization of a Nuclear Heat-Driven District Cooling System

Hussein Abdulkareem Saleh Abushamah,[1] **Ondřej Burian**,[1] **and Radek Škoda**[1,2]

[1]*Faculty of Electrical Engineering, University of West Bohemia, Univerzitni 2795/26, Pilsen, Czech Republic*
[2]*CIIRC, Czech Technical University in Prague, Praha 6, Czech Republic*

Correspondence should be addressed to Hussein Abdulkareem Saleh Abushamah; abushama@fel.zcu.cz

Received 22 December 2022; Revised 30 July 2023; Accepted 10 August 2023; Published 31 August 2023

Academic Editor: Próspero Acevedo-Peña

Carbon-free thermally driven district cooling systems (DCS) can effectively mitigate the excessive electricity consumption and carbon emissions associated with the cooling sector. This study proposes a DCS that employs nuclear heat as the primary energy source. The system comprises three main subsystems: heat station, heat transmission, and cooling station. A heat-only small modular reactor called Teplator, gas boilers, and heat storage are considered to supply the heat required to drive absorption chillers; cold storage and compression chillers are the supplementary units. The technoeconomic aspects of the system are formulated, and an algorithm is developed to determine the optimal design and operation. The method is examined for supplying a typical cooling demand profile with a peak of 2050 MW_c. The resulting optimized design includes 11 nuclear plants (150 MW_t each), 20 000 MW_th heat storage, and 1.9 m diameter heat supply/return pipes. Absorption chillers with a total capacity of 1424 MW_c are determined, covering 92% of the total cooling demand, and 244 MW_c of compression chillers and 20 000 MW_ch of cold storage are found to cover the peak and enhance the load following. This system saved 69% of the electricity consumption and carbon emissions and 34% of the costs compared with an electric-based scenario.

1. Introduction

Addressing greenhouse gas emissions is critical in tackling global warming and mitigating climate change. Consequently, it is crucial to develop low-carbon energy systems that can fulfill the energy requirements of various sectors. Globally, air conditioning in buildings accounts for nearly 20% of the building's electricity consumption. This percentage increases dramatically in hotter regions such as the Gulf countries and Central Asia, where it rises to 73% and 80%, respectively, and leads to enormous pressure on electricity grids and substantial carbon emissions. At the same time, factors such as economic growth, population increase, global warming, and urbanization are causing an unprecedented surge in global cooling energy demand. This demand is forecasted to almost triple by 2050, reaching 6,200 TWh [1–3]. Therefore, carbon-neutral thermally driven district cooling systems provide a viable solution to the main challenges the cooling sector faces: high electricity consumption and carbon emissions [4].

Inayat and Raza [5] conducted a comprehensive review of various studies that explored the application of carbon-neutral energy sources in district cooling systems. These include solar thermal energy, geothermal energy, biomass, industrial waste heat, and recovered heat from power plants. In addition, the potential of natural cooling energy sources like seas, rivers, and lakes for cooling applications has also been investigated [6]. Fangtian et al. identified two major challenges large-scale solar-driven district cooling and heating systems face: the time discrepancy between supply and demand and the spatial mismatch due to the wide area required for solar collectors. Thermal energy storage could mitigate the issue of time discrepancy. A large temperature difference between supply/return hot water could lead to cost-effective long-distance heat transmission. Therefore, solar collectors can be installed in an appropriate area far

from the demand. However, the design method they developed did not incorporate the optimization of the heat transmission pipeline [7].

Hsu et al. proposed an optimization method for designing and evaluating waste heat-driven DCSs. Their model considers the total capital and operation cost as the objective function, with the capacities of the absorption chiller and cold storage tank as objective variables. However, their optimization method is limited to local DCSs as it does not include the heat transmission infrastructures. Jannatabadi et al. [8] technoeconomically investigated a thermally driven DCS using natural gas as a heat source. Their study demonstrated its capability to significantly reduce electricity consumption in a typical hot climate region in Iran. They developed an optimizing method for determining the capacity of chillers and the chilled water distribution network.

Nuclear facilities are typically situated far from urban areas, necessitating long-distance heat transportation when utilizing nuclear heat for district heating and cooling applications. This heat may either be recovered from conventional nuclear power plants or generated by heat-only small modular reactor technologies [4]. Given that a nuclear heat-driven DCS is proposed here, the heat transmission system is an essential part that should be meticulously modeled. Safa [9] conducted a case study-based technoeconomic evaluation concerning the recovery and long-distance transportation of large-scale heat from a nuclear power plant for district heating purposes. The study demonstrated the feasibility of heat transmission over long distances (greater than 100 km). The potential economic benefits and the elimination of carbon emissions through upgrading nuclear power plants to a cogeneration mode have been evaluated for several European nuclear power plants [10]. A detailed technoeconomic model was developed to examine the feasibility of heat transportation for district heating. It was shown that the most critical factors influencing the economics of long-distance heat transmission are the heat transmission temperature, heat production or recovery cost, the price of electricity, the amount of transported thermal power, and the transmission distance [11]. In another study, the design of a heat transportation system that connects a cogeneration-operated nuclear power plant to a district heating network was optimized. The objective variables to be optimized include pipe diameter, insulation thickness, supply/return temperature, and the number of pumping stations [12].

According to the above review, nuclear heat-driven district cooling systems could provide several benefits such as saving electricity and reducing carbon emissions. However, there are several limitations and challenges that should be taken into consideration. Defining the site for nuclear facilities involves various administrative, social, environmental, and technoeconomic factors, which sometimes lead to installations located far from urban areas [13]. Therefore, it is crucial to carefully investigate the technoeconomic limitations of long-distance heat transmission, including costs, pumping requirements, heat losses, and temperature drops [11]. Moreover, certain technical challenges and constraints can limit the load-following capability of nuclear power plants [14]. In areas with low population density, district cooling systems may not be the most competitive solution due to the significant rise in capital costs for the distribution piping network [15]. Additionally, one of the main drawbacks of thermally driven refrigeration technologies is their low coefficient of performance (COP). To overcome this limitation, numerous ideas and technologies have been developed to enhance the COP of absorption-based chillers. For instance, water/lithium bromide double-effect absorption chillers offer a doubled COP (typically 1.7) compared to single-effect types (typically 0.7), but they require operation with a higher temperature heat source [16]. However, this enhancement of COP presents trade-offs that must be carefully considered, such as the impact of increased heat transmission losses and associated costs resulting from raising the temperature of the driving fluid.

This study introduces an integrated thermally driven district cooling system that comprises a heat station (containing heat generation units and storage), a bulk heat transmission (BHT) system (consisting of heat exchangers, pipeline, and pumps), and a cooling station (including chillers and cold storage). Several small modular reactor (SMR) technologies and concepts have been proposed and developed for either combined heat and power or only heat generation applications [17]. In this study, a heat-only advanced modular reactor, namely, Teplator, is considered as the primary candidate heat source. Teplator has the ability to reuse spent nuclear fuel [17, 18], with a neglectable fuel cost providing an advantageous alternative to traditional gas boilers. The candidate cooling units are absorption cycle chillers, electric compression cycle chillers, and cold storage. The BHT system transports the heat generated for driving the absorption chillers, with water serving as the heat transfer medium. An appropriate algorithm and formulations are developed to model the system and to solve its complex optimization problem within a reasonable time. The design variables and hourly operation of the system are the objective variables while ensuring technical constraints are met. The objective function is the present value of the total capital and operating costs over the decision-making period (DMP), as determined by a discounted cash flow analysis. A conceptual drawing of the proposed system is illustrated in Figure 1.

In order to identify the optimum design and hourly based operation of the proposed system, it is necessary to solve a large-scale mixed integer nonlinear programming (MINLP) problem. In this problem, the capacities and operation of all units interdependently affect each other. The main novelty of this work is the method and algorithm developed to link the main objective variables (capacities, technologies, and operation) of the heat station, heat transmission, and cooling station in one simultaneous optimization cycle. This model and algorithm can be utilized to assess the feasibility of the proposed system for various demand scales and electricity prices. Although the study introduces a nuclear heat-only reactor as the primary energy source for district cooling applications, still, the method is not confined to this technology. It can be used to evaluate various kinds of heat sources, such as geothermal energy and waste heat recovery. Furthermore, this study offers a tool for evaluating the economic feasibility and electricity

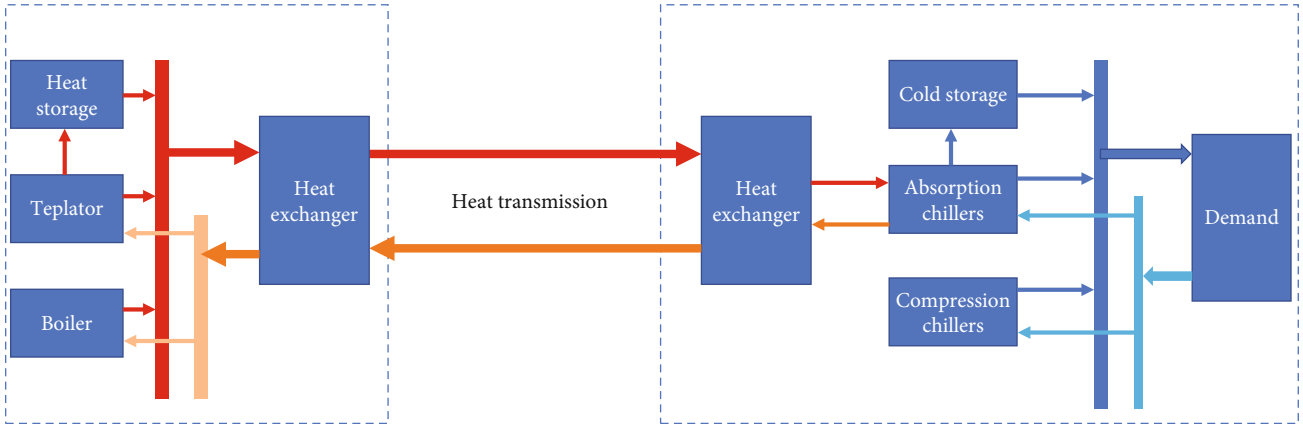

Figure 1: The conceptual illustration of the proposed system.

(and consequently, carbon emission) savings of large-scale thermally driven DCSs compared to their electric-based alternatives.

2. Method and Formulation

The objective function of the optimization expressed in (1) aims to minimize the system's total construction and hourly based operation costs while supplying a typical cooling energy demand. The initial capital costs of the heat supply station, heat transmission system, and cooling supply station represented by IC_{hss}, IC_{bht}, and IC_{css}, respectively, are determined based on their respective design capacities and technologies. The present values of the total operation and maintenance costs of these systems (OMC_{hss}, OMC_{bht}, and OMC_{css}) depend on the electricity and fuel prices as well as their operation schedules, in addition to the nominal capacities and technologies employed. At the same time, it is crucial to ensure that all technical constraints are satisfied throughout the optimization process. The solution approach is structured in three subsections. Subsection 2.1 formulates the technical limitations and design capacities, specifying the constraints that must be considered. Subsection 2.2 presents the economic equations that define the relationship between costs, design, and operation variables. Finally, Subsection 2.3 explains the solution algorithm, detailing the steps designed to find the optimal solution.

$$OF = IC_{hss} + OC_{hss} + IC_{bht} + OC_{bht} + IC_{css} + OC_{css}. \quad (1)$$

2.1. Technical Model

2.1.1. Technical Equations of the Cooling Station. The cooling station is responsible for providing the forecasted hourly cooling demand (CD^i) using a combination of the candidate units: absorption chillers (AC), electric-driven compression chillers (CC), and cold storage (CS). The cooling capacities of the AC, CC, and CS expressed by Cp_{ac}, Cp_{cc}, and Cp_{cs}, respectively, are the design variables. The operation variables are their hourly cooling power expressed by CG^i_{ac}, CG^i_{cc}, and CG^i_{cs}, respectively. To ensure adequate cooling supply, the total cooling power during any given hour (i) must meet the cooling demand at that time, according to equation (2). The cooling power generated by the chillers should not exceed their nominal capacity, as expressed in equations (3) and (4). Additionally, the hourly increase or decrease in cooling power should remain within a practical range to ensure smooth operation and prevent sudden fluctuations, as indicated in equations (5) and (6). The parameters (RR_{ac}, RR_{cc}) represent the ramp rates of the absorption and compression chillers, respectively, defined as a percentage of the nominal capacity.

$$CD^i = CG^i_{ac} + CG^i_{cc} + CG^i_{cs} \quad i = 1, \cdots, N, \quad (2)$$

$$CG^i_{ac} \le Cp_{ac} \quad i = 1, \cdots, N, \quad (3)$$

$$CG^i_{cc} \le Cp_{cc} \quad i = 1, \cdots, N, \quad (4)$$

$$CG^{i-1}_{ac} - Cp_{ac}\, RR_{ac} \le CG^i_{ac} \le CG^{i-1}_{ac} + Cp_{ac}\, RR_{ac} \quad i = 2, \cdots, N, \quad (5)$$

$$CG^{i-1}_{cc} - Cp_{cc}\, RR_{cc} \le CG^i_{cc} \le CG^{i-1}_{cc} + Cp_{cc}\, RR_{cc} \quad i = 2, \cdots, N. \quad (6)$$

The cold storage operation is subject to certain constraints given in equations (7)–(10). The negative value of the variable (CG^i_{cs}) represents the cold storage charging power, and its positive value represents the discharging power. The charging and discharging power is limited to the maximum hourly rates (RR^{ch}_{cs} and RR^{dch}_{cs}), respectively, as expressed in (7). The variable (SE^i_{cs}) represents the stored cooling energy at a specific hour (i), which can be calculated by equation (8). Obviously, the discharged power during each hour must not exceed the stored energy according to (9), and the charging power must not exceed the available free capacity of the cold storage according to (10).

$$-RR^{ch}_{cs} \le CG^i_{cs} \le RR^{dch}_{cs} \quad i = 1, \cdots, N, \quad (7)$$

$$SE^i_{cs} = SE^{i-1}_{cs} - CG^{i-1}_{cs} \quad i = 2, \cdots, N, \quad (8)$$

$$CG^i_{ac} \le SE^i_{cs}, \text{Discharging}, CG^i_{cs} > 0 \quad i = 1, \cdots, N, \quad (9)$$

$$-\mathrm{CG}_{\mathrm{cs}}^{i} \leq Cp_{\mathrm{cs}} - \mathrm{SE}_{cs}^{i}, \text{Charging}, \mathrm{CG}_{\mathrm{cs}}^{i} < 0 \quad i = 1, \cdots, N. \tag{10}$$

2.1.2. Technical Equations of the Heat Transmission System. The heat transmission system consists of a heat exchanger on the heat station side, supply/return water pipelines, pressure-boosting pumping equipment, and a heat exchanger on the cooling station side. The thermal capacity of the heat exchanger on the heat station side (Cp_{hex}) is modeled in equation (11). This capacity is designed in order to cover the thermal power required by the absorption chillers plus the losses over the transmission pipeline. In these equations, Cp_{ac} represents the total capacity of the absorption chilling technology, and $\mathrm{COP}_{\mathrm{ac}}$ denotes its average coefficient of performance. The heat transmission losses (Q^{HTL}, MWt) is estimated by equation (12) [11], where L represents the one-way length of the pipeline (m), s is the insulation thickness (mm), hi is the insulation conductivity (W/m.K), and $\Delta \mathrm{T}_{\mathrm{bht}}$ represents the temperature difference between supply and return water.

$$Cp_{\mathrm{hex}} = Q^{\mathrm{HTL}} + \frac{Cp_{\mathrm{ac}}}{COP_{\mathrm{ac}}}, \tag{11}$$

$$Q^{\mathrm{HTL}} = \frac{2 \times 10^{-6}\, \pi\, L\, \Delta \mathrm{T}_{\mathrm{bht}}\, \mathrm{hi}}{\ln\left(1 + 2(s/D)\right)}. \tag{12}$$

The heat transfer area (A_{hex}, m^2) of the heat exchanger on the heating station side, which is of the plate type, is formulated in equation (13). In this equation, (LMTD) is the logarithmic mean temperature difference which can be calculated according to (14). ΔT_A is the temperature difference between the inlet hot water and outlet cold water, and ΔT_B is the temperature difference between the outlet hot water and the inlet cold water. The heat transfer coefficient (U) in ($\mathrm{W/m^2.K}$) is a parameter of the heat exchanger [19]. Similar formulations are employed for designing the heat exchanger on the cooling station side; however, in that case, the calculations do not include the heat transmission losses.

$$\mathrm{A}_{\mathrm{hex}} = \frac{Cp_{\mathrm{hex}}}{U \cdot \mathrm{LMTD}}, \tag{13}$$

$$\mathrm{LMTD} = \frac{\Delta T_A - \Delta T_B}{\ln \Delta T_A - \ln \Delta T_B}. \tag{14}$$

The hourly transported heat (Q_{bht}^{i}, MWt) given in (15) establishes a connection between the objective variables of the cooling and heating sides. Equations (16)–(19) are used to calculate the practical range for heat transmission based on the pipe diameter. In these equations, $\dot{m}_{\mathrm{bht}}^{i}$ stands for the mass flow rate (kg/s), C_p represents the specific heat capacity of water (Ws/kg.K), ρ is the density of water ($\mathrm{kg/m^3}$), and c is the flow velocity (m/s). The thermal power transmission limits (20) associated with a given diameter are determined by assuming a feasible range for the flow velocity (19) and using equation (18). It is crucial to satisfy this constraint during the optimization process to ensure the system operates within the specified thermal power transmission limits.

$$Q_{\mathrm{bht}}^{i} = Q^{\mathrm{HTL}} + \frac{\mathrm{CG}_{\mathrm{ac}}^{i}}{\mathrm{COP}_{\mathrm{ac}}} \quad i = 1, \cdots, N, \tag{15}$$

$$Q_{\mathrm{bht}}^{i} = \frac{\dot{m}_{\mathrm{bht}}^{i}\, C_p\, \Delta \mathrm{T}_{\mathrm{bht}}}{10^6} \quad i = 1, \cdots, N\ [12], \tag{16}$$

$$\dot{m}_{\mathrm{bht}}^{i} = \rho \frac{c\, D^2}{4} \quad i = 1, \cdots, N, \tag{17}$$

$$Q_{\mathrm{bht}}^{i} = \frac{D^2\, C_p\, \Delta \mathrm{T}_{\mathrm{bht}}\, \pi\, \rho\, c}{4 \times 10^6} \quad i = 1, \cdots, N, \tag{18}$$

$$c^{\mathrm{Min}} \leq c^{i} \leq c^{\mathrm{Max}} \quad i = 1, \cdots, N, \tag{19}$$

$$Q_{\mathrm{bht}}^{\mathrm{Min}} \leq Q_{\mathrm{bht}}^{i} \leq Q_{\mathrm{bht}}^{\mathrm{Max}} \quad i = 1, \cdots, N. \tag{20}$$

Pumping power is necessary to compensate for the pressure drop caused by friction losses along the pipeline. The complex nonlinear equations given in equations (21)–(26) [20, 21] should be solved to find the hourly pumping power consumption required to balance the pressure drop. The pressure drop along the pipeline (ΔP, kPa) is formulated in (23), where (Re), the Reynolds number, calculated by equation (21).

The flow velocity ranges from 0.5 m/s to 4 m/s, while the pipe diameter ranges from 0.5 m to 2.5 m, resulting in the Reynolds numbers ranging from 850 340 to 34 013 605. When the Reynolds number exceeds 4000, the flow becomes turbulent. Therefore, to estimate the friction factor (f) in turbulent flows, the Colebrook-White equation (22) is used [21]. In these equations, Sg represents the specific gravity of water with a density of $1\ \mathrm{g/cm^3}$, and ν, and ε denote the kinematic viscosity of water and the roughness of the pipe, respectively. The required electrical pumping power (P, MWe) is formulated in (24), with (η_{ps}) representing the pump's efficiency.

Due to the nonlinearity of these equations, directly including them in the optimization would result in time-consuming calculations that may not be feasible within a reasonable time. Furthermore, the friction factor cannot be calculated directly and should be solved by iterative trial and error procedures, e.g., the Newton–Raphson [21]. To address this issue, a subprogram illustrated in Figure 2 is proposed to linearize the pumping power as a function of the transported thermal power as expressed in (25). These linear equations will be used to estimate the pumping power. The coefficients (A_D and B_D) in equation (25) can be determined using curve fitting tools for different pipe diameters. The capacity of the pumping station (Cp_{ps}) is considered as an objective variable by imposing the constraint (26) during the optimization process.

$$\mathrm{Re} = c \frac{D}{\nu}, \tag{21}$$

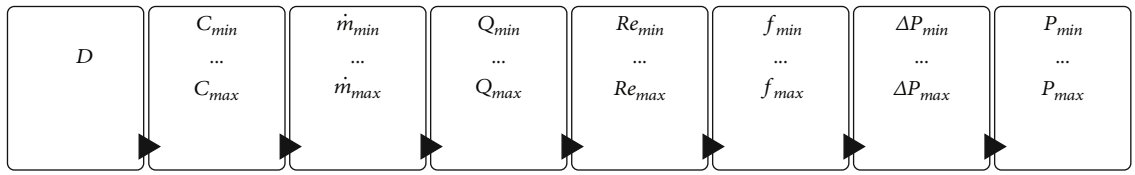

Figure 2: Linearization steps of the pumping power equation.

$$\frac{1}{\sqrt{f}} = -2\log\left(\frac{\varepsilon/D}{3.7} + \frac{2.51}{\mathrm{Re}\sqrt{f}}\right), \tag{22}$$

$$\Delta P = 0.81\, L \frac{f\,\dot{m}_{\mathrm{bht}}^2 \mathrm{Sg}}{\rho^2 D^5}, \tag{23}$$

$$P = 10^{-3}\,\dot{m}_{\mathrm{bht}} \frac{\Delta P}{\rho\,\eta_{\mathrm{ps}}}, \tag{24}$$

$$P^i = A_D\, Q_{\mathrm{bht}}^i + B_D \quad i = 1, \cdots, N, \tag{25}$$

$$Q_{\mathrm{bht}}^i \le \frac{Cp_{\mathrm{ps}} - B_D}{A_D} \quad i = 1, \cdots, N. \tag{26}$$

2.1.3. Technical Equations of the Heat Supply Station. The heat station supplies the required thermal power to drive the absorption chillers. The primary heat source utilized in this system is a nuclear heat-only reactor called Teplator, while the alternative option is gas boiler technology. Heat storage is also incorporated into the system, which can effectively contribute to peak shaving and enhance the load following. The total thermal power injected into the BHT pipeline is the combined supplied thermal power from these units, as formulated in (27) and (28) (neglecting the heat exchanger losses). This supplied thermal power must cover the thermal power requirements of the absorption chillers, in addition to the pipeline losses, as given in equation (15). In these equations, Q_{nhp}^i and Q_{gb}^irepresent the generated heat by the nuclear plants and gas boilers, respectively, and Q_{hs}^i represents the hourly charged or discharged power of the heat storage.

$$Q_{\mathrm{hss}}^i = Q_{\mathrm{nhp}}^i + Q_{\mathrm{hs}}^i + Q_{\mathrm{gb}}^i \quad i = 1, \cdots, N, \tag{27}$$

$$Q_{\mathrm{hss}}^i = Q_{\mathrm{bht}}^i \quad i = 1, \cdots, N. \tag{28}$$

The thermal output power of nuclear heat units and gas boilers is constrained to their nominal respective nominal capacity (N_{nhp}•Cp_{nhp} and Cp_{gb}), as formulated in equations (29) and (31). The variable (N_{nhp}) represents the number of nuclear plants, where each plant has a capacity of Cp_{nhp}. The hourly change in thermal power (increase or decrease) should remain within the feasible operating limits of the heat source, as specified in equations (30) and (32). The parameters ($\mathrm{RR}_{\mathrm{nhp}}$, $\mathrm{RR}_{\mathrm{gb}}$) indicate the ramp rates of the nuclear heat units and gas boilers, respectively, which are defined as a percentage of their nominal capacity.

$$Q_{\mathrm{nhp}}^i \le N_{\mathrm{nhp}} Cp_{\mathrm{nhp}} \quad i = 1, \cdots, N, \tag{29}$$

$$Q_{\mathrm{nhp}}^{i-1} - Cp_{\mathrm{nhp}}\mathrm{RR}_{\mathrm{nhp}}^{\mathrm{down}} \le Q_{\mathrm{nhp}}^i \le Q_{\mathrm{nhp}}^{i-1} + Cp_{\mathrm{nhp}}\mathrm{RR}_{\mathrm{nhp}}^{\mathrm{up}} \quad i = 2, \cdots, N, \tag{30}$$

$$Q_{\mathrm{gb}}^i \le Cp_{\mathrm{gb}} \quad i = 1, \cdots, N, \tag{31}$$

$$Q_{\mathrm{gb}}^{i-1} - Cp_{\mathrm{gb}}\,\mathrm{RR}_{\mathrm{gb}} \le Q_{\mathrm{gb}}^i \le Q_{\mathrm{gb}}^{i-1} + Cp_{\mathrm{gb}}\,\mathrm{RR}_{\mathrm{gb}} \quad i = 2, \cdots, N. \tag{32}$$

The operation of the heat storage is subject to constraints formulated in (33)–(36). The negative value of the variable (Q_{hs}^i) models the charging time, and the positive value determines the discharging mode. The charging and discharging power should not exceed the maximum hourly rates ($\mathrm{RR}_{\mathrm{hs}}^{\mathrm{ch}}$, $\mathrm{RR}_{\mathrm{hs}}^{\mathrm{dch}}$), respectively, according to (33). The variable ($\mathrm{SE}_{\mathrm{hs}}^i$) represents the stored thermal energy at each hour (i), which should satisfy the energy balance as formulated in (34) and (35). The charging power during any hour should not exceed the heat storage's free capacity at that time, according to (36). These equations govern the operation of the heat storage.

$$-\mathrm{RR}_{\mathrm{hs}}^{\mathrm{ch}} \le Q_{\mathrm{hs}}^i \le \mathrm{RR}_{\mathrm{hs}}^{\mathrm{dch}} \quad i = 1, \cdots, N, \tag{33}$$

$$\mathrm{SE}_{\mathrm{hs}}^i = \mathrm{SE}_{\mathrm{hs}}^{i-1} - Q_{\mathrm{hs}}^{i-1} \quad i = 2, \cdots, N, \tag{34}$$

$$Q_{\mathrm{hs}}^i \le \mathrm{SE}_{\mathrm{hs}}^i, \quad \text{Discharging}, Q_{\mathrm{hs}}^i > 0 \quad i = 1, \cdots, N, \tag{35}$$

$$-Q_{\mathrm{hs}}^i \le Cp_{\mathrm{hs}} - \mathrm{SE}_{\mathrm{hs}}^i, \text{Charging}, \quad Q_{\mathrm{hs}}^i < 0 \quad i = 1, \cdots, N. \tag{36}$$

2.2. Economic Model

2.2.1. Construction and Operation Costs of the Cooling Station. The costs of the system can be divided into construction and operation costs. The initial capital cost of the cooling station ($\mathrm{IC}_{\mathrm{css}}$), which includes absorption chillers, compression chillers, and cold storage, is formulated in (37). Given a large cooling demand on a city scale, it is assumed that the cooling station employs the largest commercially available size of chillers. Therefore, it is assumed that the curve of the economics of scale has reached a saturation point, meaning that further increases in chiller size would not result in considerable cost savings. Consequently, the initial capital cost of chillers is formulated per unit capacity of cooling power, where α_{ac} and α_{cc} represent the specific initial capital cost of the absorption and compression chilling units, respectively. The initial capital cost of

the cold storage (IC_{cs}) is determined by a nonlinear equation that relates to the tank size (V^s_{cs}, m^3) (38). This equation is characterized by parameters (α_{cs}, β_{cs}). The tank size itself depends on the design thermal capacity (Cp^s_{cs}), efficiency (η_{cs}), and supply/return water temperature difference (ΔT_{cs}), as expressed in (39) [22, 23]. Including this nonlinear model in the objective function increases the calculation time. A practical approach is adopted to facilitate this model, where a set of candidate capacities for the cold storage is assumed, and their corresponding initial capital costs are calculated and tabulated. During the optimization process, integer zero-one variables (x_s) are used to select the optimum option from the candidates using equation (40). In this equation, s represents the candidate number among the (M) options, and the initial capital cost of the selected one is calculated by (41).

$$\mathrm{IC}_{\mathrm{css}} = \alpha_{\mathrm{ac}}\, Cp_{\mathrm{ac}} + \alpha_{\mathrm{cc}}\, Cp_{\mathrm{cc}} + \mathrm{IC}_{\mathrm{cs}}, \tag{37}$$

$$\mathrm{IC}^s_{\mathrm{cs}} = \alpha_{\mathrm{cs}}\, (V^s_{\mathrm{cs}})^{\beta_{\mathrm{cs}}}, \tag{38}$$

$$V^s_{\mathrm{cs}} = \frac{\left(3.6 \times 10^9\right) Cp^s_{\mathrm{cs}}}{\rho\, c_p\, \eta_{\mathrm{cs}}\, \Delta T_{\mathrm{cs}}}, \tag{39}$$

$$Cp_{\mathrm{cs}} = \sum_{s=1}^{M} x_s\, Cp^s_{\mathrm{cs}} \quad x_s = 0, 1, \quad \sum x_s = 1, \tag{40}$$

$$\mathrm{IC}_{\mathrm{cs}} = \sum_{s=1}^{M} x_s\, \mathrm{IC}^s_{\mathrm{cs}} \quad x_s = 0, 1. \tag{41}$$

The annual variable and fixed O&M costs of the cooling station are formulated in (42) and (43), respectively, and their total present value ($\mathrm{OMC}_{\mathrm{css}}$) over the decision-making period is given in (44). In these equations, the parameters ($\mathrm{EC}_{\mathrm{ac}}$, $\mathrm{EC}_{\mathrm{cc}}$, EP^i, $\mathrm{SOM}^v_{\mathrm{ac}}$, $\mathrm{SOM}^v_{\mathrm{cc}}$, $\mathrm{SOM}^f_{\mathrm{ac}}$, and $\mathrm{SOM}^f_{\mathrm{cc}}$) represent the electricity consumption rates of AC and CC, electricity price, and specific variable and fixed O&M cost ($/MWh and $/MW/yr) of the units, respectively. The interest rate (IR) is used to calculate the present values. The variable O&M cost of the cold storage is considered within its annual fixed costs. The present value of the reconstruction cost ($\mathrm{RC}_{\mathrm{css}}$) is also included, which is applicable when the unit's lifetime is less than the DMP.

$$\begin{aligned}\mathrm{OM}^{\mathrm{av}}_{\mathrm{css}} = \sum_{i=1}^{N} \Big[&\left(\mathrm{CG}^i_{\mathrm{ac}}\, \mathrm{SOM}^v_{\mathrm{ac}} + \mathrm{CG}^i_{\mathrm{cc}}\, \mathrm{SOM}^v_{\mathrm{cc}}\right) \\ &+ \left(\mathrm{CG}^i_{\mathrm{ac}}\, \mathrm{EC}_{\mathrm{ac}} + \mathrm{CG}^i_{\mathrm{cc}}\, \mathrm{EC}_{\mathrm{cc}}\right) \mathrm{EP}^i \Big],\end{aligned} \tag{42}$$

$$\mathrm{OM}^{\mathrm{af}}_{\mathrm{css}} = Cp_{\mathrm{ac}} \mathrm{SOM}^f_{\mathrm{ac}} + Cp_{cc}\, \mathrm{SOM}^f_{\mathrm{cc}} + Cp_{\mathrm{cs}} \mathrm{SOM}^f_{\mathrm{cs}}, \tag{43}$$

$$\mathrm{OMC}_{\mathrm{css}} = \frac{\sum_{j=1}^{\mathrm{DMP}} \left(\mathrm{OM}^{\mathrm{av}}_{\mathrm{css}} + \mathrm{OM}^{\mathrm{af}}_{\mathrm{css}}\right)}{(1 + \mathrm{IR})^j + \mathrm{RC}_{\mathrm{css}}}. \tag{44}$$

2.2.2. Construction and Operation Costs of the BHT System. The initial capital cost of the heat transmission system is calculated by equation (45), which includes the costs associated with the pipeline and its insulation ($\mathrm{IC}_{\mathrm{pipe}}$), pressure-boosting pumps ($\mathrm{IC}_{\mathrm{pump}}$), and heat exchangers at the heat station and cooling station sides ($\mathrm{IC}^{\mathrm{hss}}_{\mathrm{hex}}$, $\mathrm{IC}^{\mathrm{css}}_{\mathrm{hex}}$).

$$IC_{bht} = \mathrm{IC}_{\mathrm{pipe}} + \mathrm{IC}_{\mathrm{pump}} + \mathrm{IC}^{\mathrm{hss}}_{\mathrm{hex}} + \mathrm{IC}^{\mathrm{css}}_{\mathrm{hex}}. \tag{45}$$

The capital cost of the pipeline, which has a one-way length of (L, m), is determined using the formulations proposed by [24]. The outer diameter of the pipe (D_{out}) is calculated according to equation (46), and the weight of the pipe ($\mathrm{Wt}_{\mathrm{pipe}}$) is given in (47). The parameters ($K1$, $K2$, $W1$, $W2$, and $W3$) depend on the pipe's thickness and material. The required volume of the insulation (V_{ins}) is calculated using equation (48) [11]. The initial capital cost of the pipe is then calculated by equation (49), where α_{pipe} represents the cost of the pipe material ($/kg), β_{pipe} is associated with installation costs, γ_{pipe} represents the right-of-way costs, and δ_{pipe} stands for the cost of the insulation ($/$m^3$).

$$D_{\mathrm{out}} = K1\, D_{\mathrm{in}} + K2, \tag{46}$$

$$\mathrm{Wt}_{\mathrm{pipe}} = W1\, D^2_{\mathrm{in}} + W2\, D_{\mathrm{in}} + W3, \tag{47}$$

$$V_{\mathrm{ins}} = \left(\frac{\pi}{4}\right) \left[(D_{\mathrm{in}} + s)^2 - s^2\right] 10^{-6}, \tag{48}$$

$$\mathrm{IC}_{\mathrm{pipe}} = 2\, L \left(\alpha_{\mathrm{pipe}}\, \mathrm{Wt}_{\mathrm{pipe}} + \beta_{\mathrm{pipe}}\, D^{0.48}_{\mathrm{out}} + \gamma_{\mathrm{pipe}} + \delta_{\mathrm{pipe}}\, V_{\mathrm{ins}}\right). \tag{49}$$

The capital cost of the pump ($\mathrm{IC}_{\mathrm{pump}}$) is modeled as a linear function of the nominal capacity in (50). The present value of the BHT operation cost over the decision-making period is formulated in (51), where P^i represents the hourly electricity consumption formulated in (25), EP^i is the electricity price, and IR is the annual interest rate. The pressure drop is assumed to be the same for both the supply and return pipes. The present value of the cost of the pipe reconstruction ($\mathrm{RC}_{\mathrm{bht}}$) is also included, which may be required during the DMP.

$$\mathrm{IC}_{\mathrm{pump}} = 2\, \alpha_{\mathrm{pump}}\, Cp_{\mathrm{pump}}, \tag{50}$$

$$\mathrm{OMC}_{\mathrm{bht}} = 2 \sum_{j=1}^{\mathrm{DMP}} \sum_{i=1}^{N} P^i\, \mathrm{EP}^i\, (1 + \mathrm{IR})^{-j} + \mathrm{RC}_{\mathrm{bht}}. \tag{51}$$

The initial capital cost of the heat exchanger ($\mathrm{IC}_{\mathrm{hex}}$) is given in (52), which has the cost parameters ($\alpha_{\mathrm{Hex}}, \beta_{\mathrm{Hex}}, \gamma_{\mathrm{Hex}}$). This equation is used for both heat exchangers on the heating and cooling station sides. The design areas (A_{hex}) of these heat exchangers are calculated using equation (13) in Subsection 2.1.1.

$$\mathrm{IC}_{\mathrm{hex}} = \alpha_{\mathrm{Hex}}\, (\beta_{\mathrm{Hex}} + \gamma_{\mathrm{Hex}}\, A_{\mathrm{hex}}). \tag{52}$$

2.2.3. Construction and Operation Costs of the Heat Supply Station. The number of nuclear plants (N_{nhp}), the capacities of the gas boilers (Cp_{gb}) and heat storage (Cp_{hs}) are considered objective variables to be optimized. The total capital

Table 1: Objective variables.

Design variables					
Group A		Group B			
Symbol	Definition	Symbol	Definition		
T^s_{hs}	Heat station supply temperature.	N_{nhp}	Number of nuclear heat plants.		
T^r_{hs}	Heat station return temperature.	Cp_{hs}	Capacity of heat storage.		
T^s_{bht}	Supply temperature of BHT.	Cp_{cs}	Capacity of cold storage.		
T^r_{bht}	Return temperature of BHT.	Cp_{gb}	Capacity of gas boiler unit.		
D	Inner diameter of transmission pipeline.	Cp_{ac}	Capacity of absorption chillers.		
s	Insulation thickness of the pipeline.	Cp_{cc}	Capacity of compression chillers.		
		Cp_{hex}	Capacity of heat exchangers.		
Group C: Operation variables					
Q^i_{nhp}	Hourly thermal power of nuclear plants.	Q^i_{gb}	Hourly thermal power of gas boilers.	Q^i_{hs}	Hourly thermal power of heat storage.
C^i_{ac}	Hourly cooling power of absorption chillers.	C^i_{cc}	Hourly cooling power of compression chillers.	C^i_{cs}	Hourly cooling power of cold storage.

cost of these units is given in (53). A similar approach and formulation as those used for the capital cost estimation of cold storage in equations (38)–(41) are applied here to calculate the heat storage capital cost (IC_{hs}). The initial capital cost of the nuclear plants (IC_{nhp}) is a discrete function of the number of nuclear plants, where α_{nhp} represents the one-plant capital cost. The capital cost of the gas boiler is a continuous linear function of the boiler's capacity, where α_{gb} is the specific capital cost per thermal MW.

$$IC_{hss} = \alpha_{nhp} N_{nhp} + \alpha_{gb} Cp_{gb} + IC_{hs}. \tag{53}$$

The annual variable and fixed O&M costs of the heat station are calculated by equations (54) and (55), respectively, and their total present value is given by equation (56). In these equations, Q^i represents the hourly thermal power, and the subscripts (hss, nhp, gb, hs) refer to the heat supply station, nuclear heat units, gas boiler, and heat storage, respectively. The superscripts $(a, v, f,)$ denote annual, variable, and fixed costs, respectively. The abbreviations SFC and SOM stand for the specific fuel cost and specific O&M costs ($/MWh), while EC and EP represent the electricity consumption rate and electricity price, respectively. The present value of the reconstruction cost of the heat station (RC_{hss}) is included when the unit's lifetime is shorter than the DMP.

$$\begin{aligned} OM^{av}_{hss} = {} & \sum_{i=1}^{N} Q^i_{nhp} \left[\left(SFC_{nhp} + SOM^v_{nhp} \right) + EC_{nhp}\, EP^i \right] \\ & + Q^i_{gb} \left[\left(SFC_{gb} + SOM^v_{gb} \right) + EC_{gb}\, EP^i \right], \end{aligned} \tag{54}$$

$$OM^{af}_{hss} = Cp_{nhp}\, SOM^f_{nhp} + Cp_{gb}\, SOM^f_{gb} + Cp_{hs}\, SOM^f_{hs}, \tag{55}$$

$$OMC_{hss} = \sum_{j=1}^{DMP} \left(OM^{av}_{hss} + OM^{af}_{hss} \right) / (1 + IR)^j + RC_{hss}. \tag{56}$$

2.3. Solution Algorithm. The optimization of the proposed district cooling system is a complex problem that involves various interdependent variables and constraints. The presence of both integer and continuous variables, combined with the nonlinearity of the equations, adds further complexity to the optimization process. Therefore, a unique algorithm is developed to solve this MINLP problem within a reasonable time effectively.

Upon reviewing the formulations, it becomes evident that certain variables play a crucial role in the complexity of the problem. These variables include the diameter of the pipeline (D) and its insulation (s), the temperature differences across the system (ΔT), the number of the nuclear plants (N_{nhp}), and the capacity of the thermal energy storages (Cp_{hs} and Cp_{cs}). To facilitate the optimization process in a systematic approach, the design variables are categorized into two groups, along with the operation variables addressed in Table 1.

The optimization process is structured in several steps, illustrated in Figure 3. Step 1 involves gathering the necessary input data, such as the demand data, electricity and fuel prices, technoeconomic parameters of the system, and candidate options for the objective variables. In step 2, a set of M candidate solutions is generated, assigning values to the variables in group A (such as D and s). These values are then applied to all the technoeconomic equations of the system, directly resulting in the linearization and simplification of several equations in step 3. In step 4, the linearization of the pumping power and its cost calculation is performed. As a result, a mixed integer linear optimization problem remains, which can be efficiently solved in step 5. Here, the variables in group B, along with the operational variables

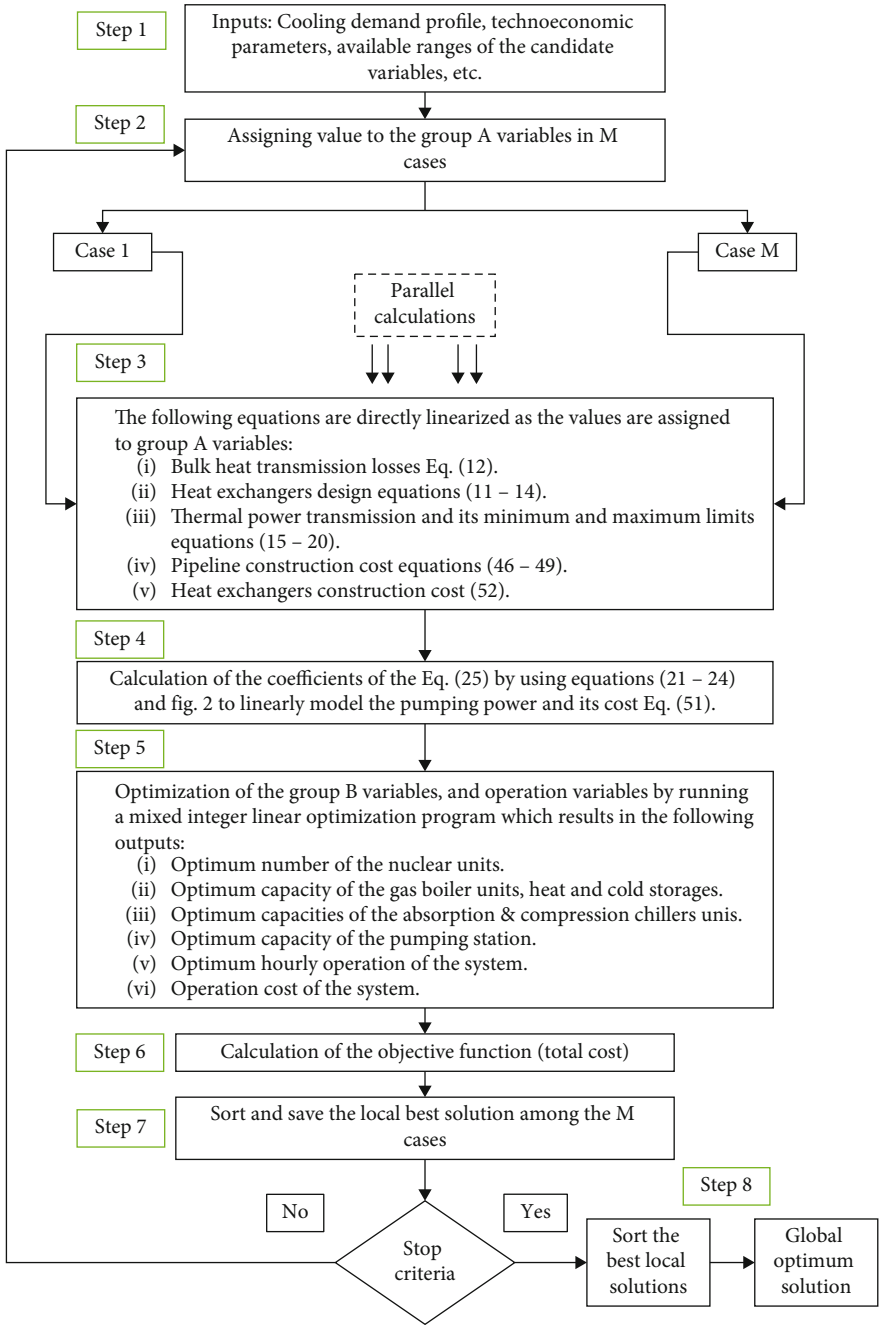

Figure 3: The proposed algorithm for the optimization process.

in group C, are optimized. The objective function is calculated, and the local optimum solution among the M cases is saved in step 6. The calculation cycle continues from step 2, generating new M cases for the variables in group A. This repetitive process continues until all possible candidate solutions have been evaluated, ultimately determining the optimum solution in steps 7 and 8.

3. Case Study

To examine the optimization method, this study utilizes the one-year hourly cooling demand profile of Qatar, which was previously modeled and reported by Alghool et al. [25]. This demand profile, with a peak of 4100 MW_c, is scaled down by 50% to a peak of 2050 MW_c for the case study conducted here. The objective is to optimize the proposed system to meet this scaled-down demand. Teplator, the primary candidate heat source, can supply hot water within a temperature range of (98–200°C) [18]. This case study considers a single-effect lithium bromide solution-based absorption technology that operates with hot water at 95°C. This technology is among the most common and practical types available [26, 27]. Therefore, specific temperature values are predetermined and indicated in Figure 4 and Table 2 to ensure

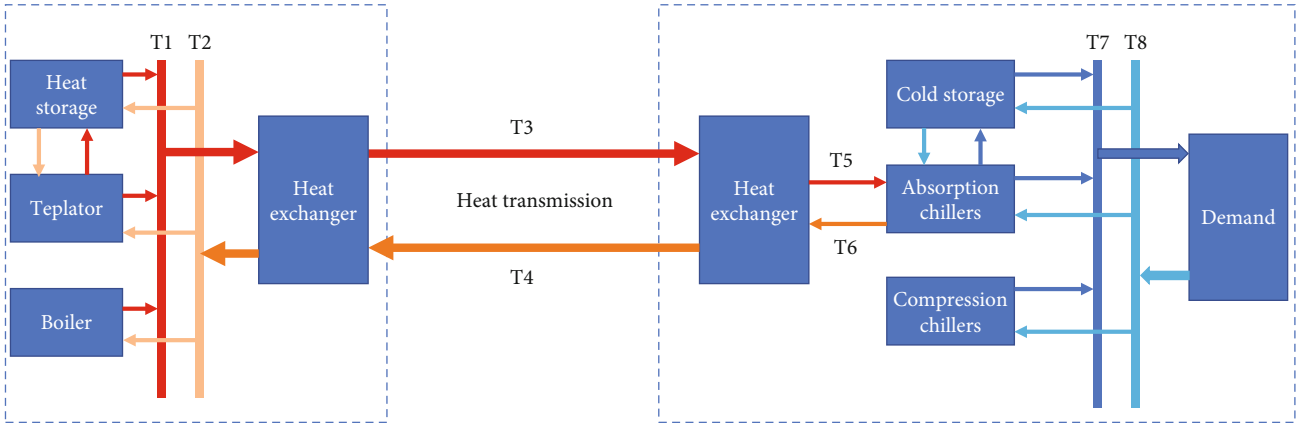

Figure 4: The system's temperature indication.

Table 2: The assumed temperatures in the system.

Heat station supply/return temperatures (°C)	T1/T2	170/90	Temperatures of supply/return hot water driving absorption chillers (°C)	T5/T6	95/55
Transmission supply/return temperatures (°C)	T3/T4	120/70	Temperatures of supply/return chilled water (°C)	T7/T8	5/13

compatibility with these technologies. Although the temperatures are predetermined for this typical case study, the same algorithm can be applied when exploring alternative heat generation options (e.g., higher temperature sources) and different absorption chilling technologies (e.g., double effect). The designed algorithm incorporates a parallel calculation feature, enabling efficient solution finding within a reasonable time.

The physical and technical parameters used in the calculations are given in Table 3. For the heat transmission system, it is assumed that the heat station is located 20 km away from the cooling station. Consequently, the total length of the supply/return hot water pipe is 40 km. A recommended flow velocity range of 0.5 m/s–4 m/s is considered to ensure proper system operation and avoid potential damages such as mechanical stress and erosion [9]. Plate-type heat exchangers are considered to be installed on both sides of the pipeline: one receives heat from the heat station, and the other delivers it to the absorption cooling units. These heat exchangers are assumed to have similar specifications. The overall heat transfer coefficient for water-to-water heat exchangers is reported to be in the range (850-1700 W/(m K)) [28]. This case study assumes a typical value of 1500 W/(m K) as the overall heat transfer coefficient.

The power ramp rates of the heat and cold supply units are crucial for effective load following in the system. The hourly change in nuclear power is restricted within a range of +10% and -5% of the nominal unit's capacity to ensure smooth operation. This study neglects thermal storage losses due to their minimal impact, as weekly losses are estimated to be only 1% for a 5000 m^3 tank, and the roundtrip efficiency is about 98% [23].

Table 4 provides the candidate solutions for the design variables considered in this study. It includes the candidate numbers of nuclear plants, with each unit having a capacity of 150 MWt, as well as the candidate capacities of the gas boiler, absorption chillers, and compression chiller. The candidate capacities are assumed within a wide range up to the peak demand. Furthermore, various candidate diameters are assumed for the heat transmission pipeline, allowing for flexibility in system design. In terms of insulation, a single option is considered for the type and thickness to simplify the calculations. Limiting the insulation options puts the focus on other critical variables.

The values of the design variables are accepted as optimal when they result in the minimum total cost while satisfying the technical constraints. The objective function, which encompasses the total capital and operation cost, is calculated using the economic parameters addressed in Table 5. For the calculations, electricity and gas prices are assumed to be 144 $/MWeh and 41 $/MWth, respectively. These values correspond to the average nonhousehold consumer prices in the European Union [31] [32].

4. Results

4.1. Base Scenario. A base scenario introduced is an entirely electric-driven district cooling system utilizing compression chillers and cold storage to be compared to the proposed system. This system is optimized to efficiently supply a one-year hourly cooling demand with a peak of 2050 MWc. The optimized system's capacities and corresponding capital and O&M costs are addressed in Table 6. The O&M cost of the compression chillers, mainly associated with electricity consumption, constitutes 85% of the total cost. Among the options for cold storage (referenced in Table 4), the most suitable choice is the largest one, with a capacity of 20,000 MWh. The total capacity of the chillers is 1668 MWc, less than the peak demand (2050 MW). Therefore, the cold storage effectively covered 382 MWc of the peak demand.

Table 3: Physical and technical parameters of the system.

System	Parameter	Symbol	Value	Ref.
Heat transfer fluid: water	Density (kg/m3)	ρ	958	[12]
	Specific heat capacity (J/kg. K)	C_p	4220	[12]
	Kinematic viscosity (m^2/s)	ν	0.294×10^{-6}	—
Heat transmission	Distance between heat station and chilling station (m)	L	20 000	—
	Weight and outer diameter calculation parameters of the schedule 80 steel pipe (equations (46) and (47))	$K1$ $K2$ (m) $W1$ (kg/m^3) $W2$ (kg/m^2) $W3$ (kg/m)	1.101 0.006349 1330 75.18 0.9268	[20]
	Maximum flow velocity (m/s)	c^{Max}	4	[9]
	Minimum flow velocity (m/s)	c^{Min}	0.5	—
	Pump efficiency	η_P	75%	[12]
	Lifetime of pipeline	$\mathrm{LT_{TP}}$	50	[12]
Heat exchangers	Overall heat transfer coefficient W/(m K)	U	1500	[28]
	Efficiency	η_{hex}	80%	[12]
	Lifetime of heat exchanger	$\mathrm{LT_{hex}}$	25	
Teplator	Increasing power ramp rate (MW/hr)	$\mathrm{RR_{nhp}^{up}}$	±10%	—
	Decreasing power ramp rate (MW/hr)	$\mathrm{RR_{nhp}^{down}}$	±5%	—
	Electricity consumption (MWeh/MWth)	$\mathrm{EC_{nhp}}$	1%	—
	Lifetime of Teplator (year)	$\mathrm{LT_{nhp}}$	50	
Gas boiler	Power ramp rate (MW/hr)	$\mathrm{RR_{gb}}$	±100%	—
	Electricity consumption (MWeh/MWth)	$\mathrm{EC_{gb}}$	0.14%	[29]
	Efficiency	η_{gb}	103%	[29]
	Lifetime of gas boiler (year)	$\mathrm{LT_{gb}}$	25	[29]
Heat storage	Charging/discharging power (MWt/hr)	$\mathrm{RR_{hs}}$	2% of the capacity	—
	Electricity consumption (MWeh/MWth)	$\mathrm{EC_{hs}}$	1%	[23]
	Charging/discharging efficiency	η_{hs}	100%	[23]
	Lifetime of heat storage	$\mathrm{LT_{hs}}$	50	—
Cold storage	Charging/discharging power (MWc/hr)	$\mathrm{RR_{cs}}$	2% of the capacity	—
	Electricity consumption (MWeh/MWch)	$\mathrm{EC_{cs}}$	1%	—
	Charging/discharging efficiency	η_{cs}	100%	—
	Lifetime of cold storage (year)	$\mathrm{LT_{cs}}$	50	—
Absorption chiller	Power ramp rate (MWc/hr)	$\mathrm{RR_{ac}}$	±20%	—
	Electricity consumption (MWeh/MWch)	$\mathrm{EC_{ac}}$	5%	—
	Average COP	$\mathrm{COP_{ac}}$	0.85	[30]
	Lifetime of absorption chillers (year)	$\mathrm{LT_{ac}}$	25	—
Compression chiller	Power ramp rate (MWc/hr)	$\mathrm{RR_{cc}}$	±20%	—
	Electricity consumption (MWeh/MWch)	$\mathrm{EC_{cc}}$	27%	—
	Average COP	$\mathrm{COP_{cc}}$	4	—
	Lifetime of compression chillers (year)	$\mathrm{LT_{cc}}$	25	—

Table 4: Candidate options for design variables.

	Variable	Symbol	Value
Heat station variables	Number of nuclear plants	N_{nhp}	0–14
	Capacity of heat storage (MWth)	Cp_{hs}	(0, 2000, 4000, 8000, 12 000, 20 000)
	Capacity of gas boiler (MWt)	Cp_{gb}	0–peak thermal demand
Heat transmission variables	Pipe diameter (m)	D_{in}	(0, 0.5, 0.7, 1, 1.2, 1.5, 1.7, 1.9, 2, 2.1, 2.2, 2.5)
	Pipe (iron) absolute roughness (mm)	ε	0.2
	Insulation type: thermal conductivity (W/m.K)	hi	0.03
	Insulation thickness (mm)	s	200
Chilling station variables	Capacity of absorption chilling (MWc)	Cp_{ac}	0–peak cooling demand
	Capacity of compression chilling (MWc)	Cp_{cc}	0–peak cooling demand
	Capacity of cold storage (MWch)	Cp_{cs}	(0, 2000, 4000, 8000, 12 000, 20 000)

Table 5: Construction and operation cost factors.

	System	Construction cost	Annual fixed O&M cost	Variable O&M cost
Cooling station	Absorption chiller (37) [4]	$\alpha_{ac} = 801\,000$ (€/MWc)	13 380 (€/MWc/yr)	—
	Compression chiller (37) [4]	$\alpha_{cc} = 590\,000$ (€/MWc)	37 390 (€/MWc/yr)	—
	Cold storage (38)	$\alpha_{cs} = 7450$ (€/m^3) $\beta_{cs} = 0.53$	8.6 (€/MWch/yr)	0
Heat transmission system	Pipeline (equation (49)) [11] [24]	$\alpha_{pipe} = 0.82$ (€/kg) $\beta_{pipe} = 185$ (€/kg$^{0.48}$) $\gamma_{pipe} = 6.8$ (€/m) $\delta_{pipe} = 110$ (€/m^3) (polyurethane foam insulation)	0.04% of the capital cost	0
	Pump (equation (50)) [20]	$\alpha_{pump} = 1000$ \$/MWe (€)	Included in the pipeline FO&M cost	Table 6 equation (50)
	Heat exchanger (equation (52))	$\alpha_{hex} = 1$ $\beta_{hex} = 11\,000$ (€) $\gamma_{hex} = 150$ (€/m^2)	Included in the pipeline FO&M cost	0
Heat station	Teplator (53) [18] [33]	$\alpha_{nhp} = 30\,000\,000$ (€)	18 000 (€/MWt/yr)	1 (€/MWth)
	Gas boiler (53) [29]	$\alpha_{gb} = 50\,000$ (€/MWt)	1900 (€/MWt/yr)	0.9 (€/MWth)
	Heat storage (38) [23]	$\alpha_{hs} = 7450$ (€/m^3) $\beta_{hs} = 0.53$	8.6 (€/MWth/yr)	0

4.2. The Proposed System. After evaluating the electric-driven scenario discussed in the previous subsection, we here present the optimization results for the thermally driven DCS. Before initiating the optimization cycle, several constraints and parameters are calculated. Table 7 presents the calculated coefficients for the linear equations that model the one-way water transmission pumping power, as well as the heat transmission constraints and heat station shutdown periods associated with each pipe diameter. The minimum and maximum thermal power transmissions for each diameter are associated with the feasible flow velocity range of 0.5 m/s–4 m/s). When the required thermal power to operate the absorption chillers falls below the minimum transmission limit due to low cooling demand, the heat station will be temporarily out of service. Therefore, the heat station shutdown periods are considered in the optimization process. The data given in Table 7 indicate that larger pipes have larger minimum and maximum heat transmission limits. As a result, when larger pipes are employed in the system, they have the capacity to cover a higher cooling demand during peak times. However, they lead to an extension in the duration during which the low cooling demand cannot be met. There is another tradeoff between pumping power and the capital cost of the pipe. Using a larger pipe to transport the same amount of thermal power results in reduced pumping power requirements; in contrast, it comes with an increased initial capital cost for the pipe.

Table 6: The achieved design capacities and costs associated with the base scenario.

			Optimum design capacity	Annual O&M cost (M$)	Present value of O&M cost over DMP (M$)	Capital cost (M$)
Chilling station	Compression chilling	Cp_{cc}	1668 MWc	322.92	6937.1	1168.7
	Cold storage	Cp_{cs}	20 000 MWch/400 MW	0.172	3.695	17.233
Total capital and operation cost of the system:				323.1	6940.8 8126.7 M$	1185.9

Table 7: Linearized pumping power coefficients, thermal power transportation limits, and shutdown periods of heat station associated with the pipe diameters.

D (m)	$P^i = A_D Q^i_{bht} + B_D$ (26) Based on a 20 km distance		Minimum thermal power (MW)	Maximum thermal power (MW)	Heat station and transmission hourly shutdown periods over a year due to low demand and transmission limit.			
	A_D	B_D			From	To	From	To
0.5	0.0298	-1.6116	20	159	1	744	—	—
0.7	0.0198	-2.0988	39	311	1	1433	8187	8784
1	0.0129	-2.7845	79	635	1	1440	8041	8784
1.2	0.0103	-3.2208	114	914	1	1440	8041	8784
1.5	0.0079	-3.8523	179	1429	1	2166	8041	8784
1.7	0.0068	-4.261	229	1835	1	2184	8041	8784
1.9	0.006	-4.6616	287	2293	1	2214	8041	8784
2	0.0056	-4.8592	318	2540	1	2262	8041	8784
2.1	0.0053	-5.0552	350	2800	1	2598	8041	8784
2.2	0.005	-5.2496	384	3074	1	2766	8041	8784
2.5	0.0043	-5.8243	496	3969	1	2898	7326	8784

Table 8 presents the achieved optimum design capacities for the system proposed in this study. In the optimized configuration, absorption chillers cover approximately 70% of the peak cooling demand, while electric-driven compression chillers contribute only 12%. Additionally, cold storage plays an important role in covering 18% of the peak cooling demand. The heat station incorporates eleven nuclear plants (Teplator) with a combined thermal capacity of 1650 MW to supply the thermal power required for driving the absorption chillers. Among the assumed options for thermal storages, the larger ones are selected as heat and cold storages, emphasizing their cost-effective role in this system. The optimized system employs supply/return heat transmission pipes with an optimal inner diameter of 1.9 m. Each supply and return pipe requires a total pumping power of (5.4 MW). The thermal capacity of heat exchanger-1 (on the heating side) is 1675 MW, which transfers heat from the heating station to the transmission pipeline cycle. Heat exchanger-2, with a capacity of 1650 MW, transfers thermal power from the transmission cycle to the absorption chillers.

Although the proposed system has a capital cost that is 77% higher than the base scenario (Table 6), its considerably lower operation cost makes it a more cost-effective solution. The present value of the total cost of the optimized system is nearly 34% less than the cost of the base electric-driven system. It is important to note that these cost calculations are based on a 4% interest rate, and different optimum solutions may arise when considering higher interest rates.

According to the energy balance calculations outlined in Table 9, absorption chillers fulfill approximately 92% of the annual cooling energy demand, while compression chillers provide only 7%. Consequently, the optimized system significantly reduced the annual electricity consumption by 69% compared to the base electric-driven scenario, which reflects a significant carbon elimination.

Figure 5 illustrates the cost of the optimized system associated with various pipe diameters assumed in Table 4. While it was technically feasible to transport 1675 MW of heat using a 1.7 m diameter pipe (as indicated in Table 7), according to the fitted curve, the 1.8 m diameter pipe emerged as a slightly superior solution. This is due to the lower pumping cost associated with the 1.8 m diameter pipe, which offset its higher capital cost.

Figure 6 provides a visual representation of the optimum hourly operation of the cooling station. It demonstrates that cold storage and compression chillers play a crucial role when the cooling demand is low, particularly when the thermal power required to drive the absorption chillers falls below the minimum heat transmission limit. During these periods, the utilization of cold storage and compression chillers becomes necessary to ensure a sufficient cooling supply. Moreover, they effectively contribute to peak shaving

Table 8: The optimized design capacities and achieved costs for the proposed system.

		Symbol	Optimum design variable	Annual operation cost (M$)	Present value of operation cost over DMP (M$)	Capital cost (M$)
Heat station	Nuclear plants	N_{nhu}	11 ($11 \times 150 = 1650$ MW)	47.5	1020.3	330
	Heat storage	Cp_{hs}	20 000 MWth/400 MW	0.17	3.69	6.52
	Gas boiler	Cp_{gb}	0	0.00	0	0
Heat transmission	Heat exchanger 1	Cp_{hex} A_{hex}	1675 MW 33 597 m^2	6.92	148.68	6
	Heat exchanger 2	Cp_{hex} A_{hex}	1650 MW 57 057 m^2			10.18
	Pipe	D_{in}	1.9 m			173.03
	Insulation	s	200 mm			6.35
	Pumps	Cp_{pump}	2×5.4 MWe	6.42	138	19.32
Cooling station	Absorption chilling	Cp_{ac}	1424 MWc	63.77	1369.6	1354.7
	Compression chilling	Cp_{cc}	244 MWc	28.02	608	170.91
	Cold storage	Cp_{cs}	20 000 MWch/400 MWc	0.17	3.69	17.23
The total cost of the optimum design and operation of the system				152.97	3292 5386.2 M$	2094.2

Table 9: Energy balance of the system.

Annual energy balance	Proposed system				Electric-driven system
Heat generation (TWh)	Teplator: 7.294			Heat storage (fully charged in advance): 0.02	0
Electricity consumption (GWh)	Teplator	Pumping	Absorption chillers	Compression chillers	Compression chillers
	72.94	44.614	310.41	133.2	1809.4
	Total: 561.16				
Cooling generation (TWh)	Absorption chillers	Compression chillers		Cold storage (fully charged in advance)	Compression chillers + precharged cold storage
	6.2081	0.4933		0.02	(6.7015 + 0.02)
Total cooling demand (TWh)	6.7215				

and enhancing load following. By incorporating this supplementary equipment, the DCS becomes more adaptable and capable of responding to fluctuations in cooling demand, ultimately leading to a more reliable operation.

4.3. Sensitivity Analysis. The reported results in Table 6 show that the economics of the electric-driven scenario is highly influenced by its operation costs, mainly due to the high electricity price and significant electricity consumption rate. The sensitivity analysis on electricity price, as illustrated in Figure 7, confirms that the proposed thermally driven system becomes more competitive than the electric-driven system as the electricity price increases and vice versa. However, even with a considerable reduction in electricity price (e.g., 60%), the proposed thermally driven system remains the optimum solution in several cases. This sensitivity analysis also shows that the optimum diameter of the heat transmission pipe is not significantly influenced by electricity price. The pipe diameter remains within the range of 1.7 m–2 m for several cases, as shown in Figure 7.

Another sensitivity analysis, illustrated in Figure 8, evaluates the proposed system considering different distances between the heat generation and cooling stations, assuming a fixed transmission pipe diameter of 1.7 m. When the electricity price is relatively high (e.g., 144 $/MWh), the proposed thermally driven system seems economically viable even for distances of up to 130 km. On the other hand, the electric-driven scenario is more cost-effective when the electricity price is relatively low (e.g., 43 $/MWh). This is particularly true in situations where the thermally-driven system requires a heat transmission distance exceeding 25 km.

The proposed methodology and algorithm in this study have been implemented using MATLAB. The reliability of the algorithm and the accuracy of the results are well-

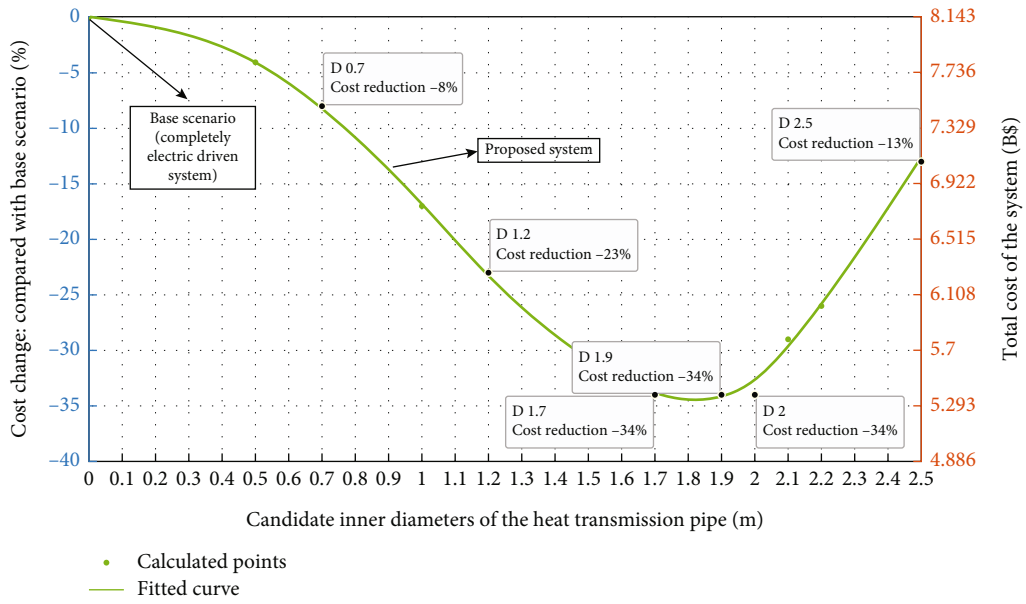

Figure 5: The total cost of the optimized system corresponding to heat transmission pipe diameters (for a 20 km distance case).

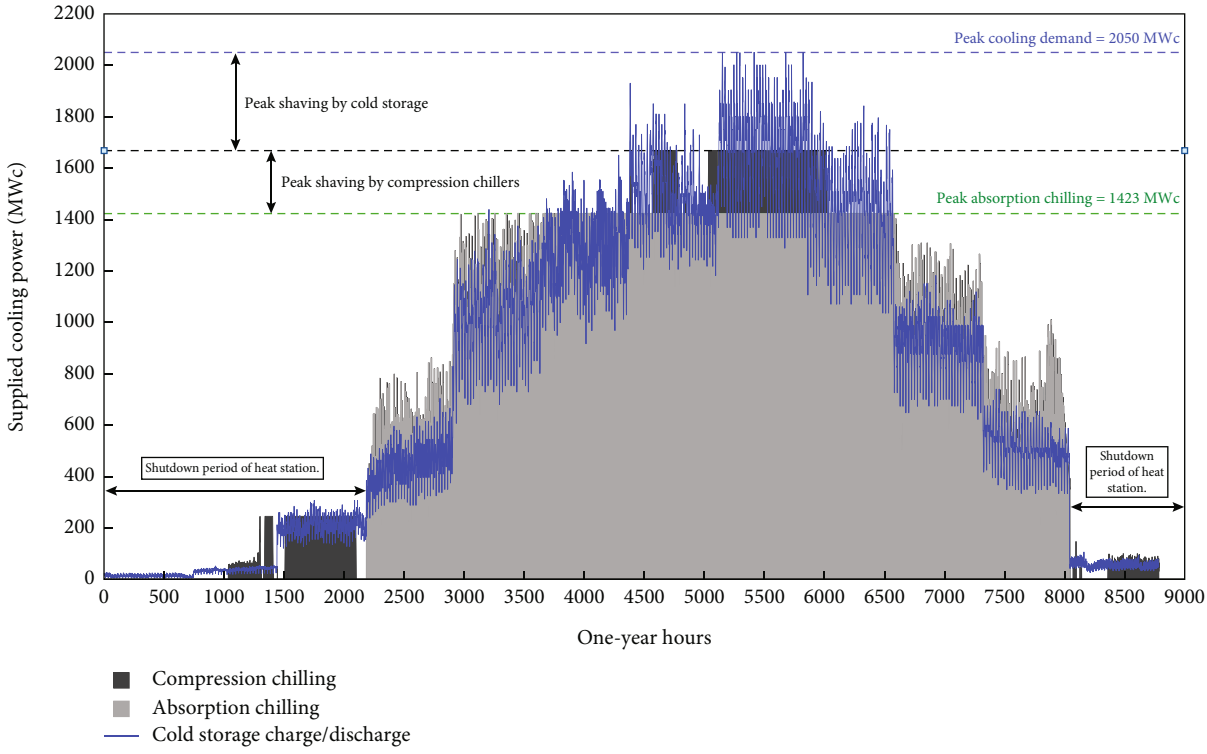

Figure 6: Optimized operation scheduling of the cooling station.

founded. The algorithm employs a comprehensive searching method that evaluates all predefined candidate options for the group A variables, such as the diameter of the pipeline (as evident in Figure 2, which clearly illustrates the optimum diameter value among the candidate range). Moreover, in each iteration associated with the selected options for variables belonging to group A, the robust mixed-integer linear programming function, "intlinprogin" in MATLAB, is employed. This function aids in finding the optimum variables of group B and the operation variables, contributing to the effectiveness and efficiency of the optimization process. In-depth analysis of the results confirms that the defined constraints are fully satisfied, and the design capacities fall within the predetermined ranges. For instance, the energy balance is successfully achieved, as demonstrated in Table 9, and the load-following capability is aptly portrayed

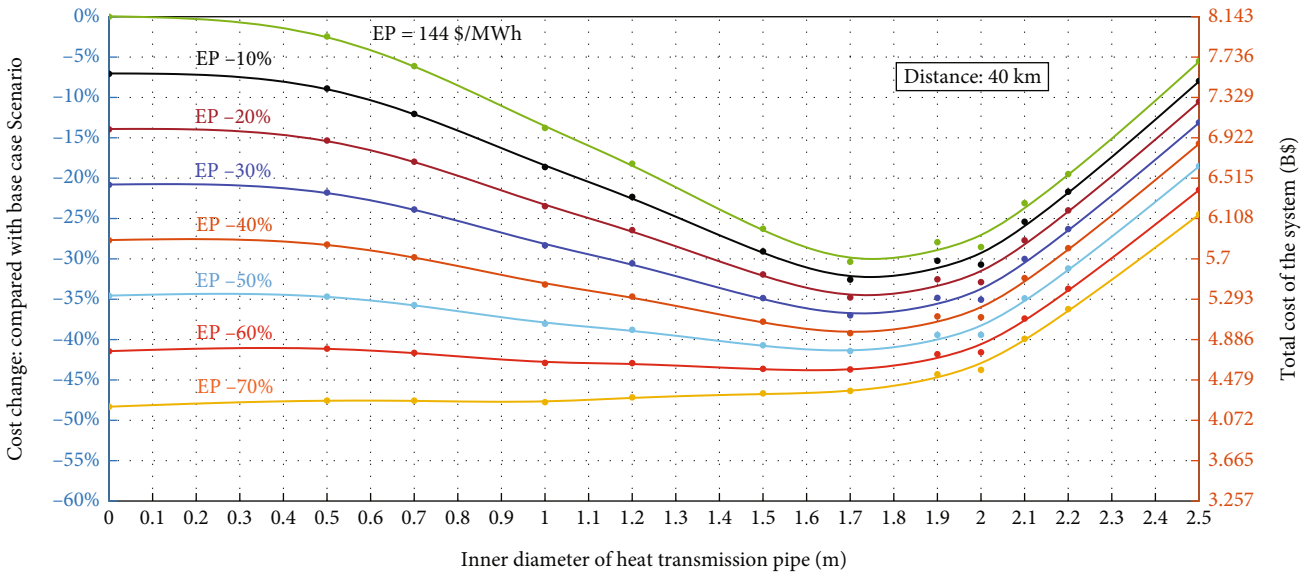

Figure 7: Sensitivity to electricity price.

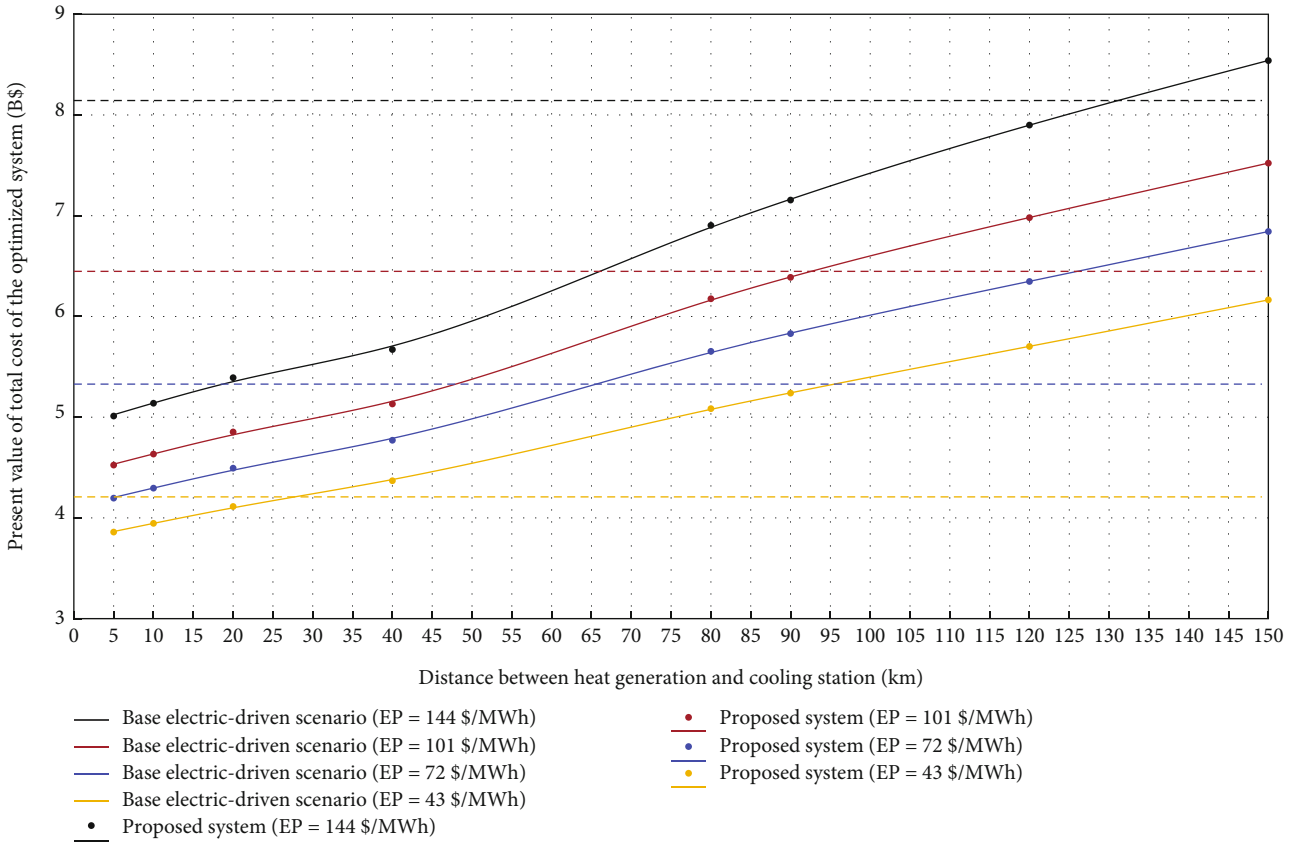

Figure 8: The proposed system's cost sensitivity to distance and electricity price compared to the base scenario.

in Figure 6. Furthermore, the resulting optimum design capacities, as presented in Table 8, align with the available options determined in Table 4. Additionally, the sensitivity analysis, depicted in Figures 7 and 8, aligns with logical expectations. For instance, increasing the distance and electricity price indeed impact the economics of the proposed thermally driven system, and the sensitivity analysis accurately captures these dynamics. In summary, the use of MATLAB and the thorough evaluation of the results demonstrate the robustness and accuracy of the proposed methodology, contributing to the credibility and validity of our findings.

5. Conclusions

This study proposes an integrated district cooling system primarily powered by nuclear heat and develops an optimization method for its design and operation. The system consists of three main parts: a heat station, a heat transmission system, and a cooling station. The heat supply options include a heat-only SMR called Teplator, gas boilers, and heat storage. The diameter of the pipe used for heat transmission is a crucial variable in the system design. Cooling equipment options are absorption chillers, compression chillers, and cold storage. The objective is to minimize the total cost, and the decision-making variables involve the design capacities, technology selection, and hourly operation of the main components. The system is optimized to supply a typical large-scale cooling demand with a peak demand of 2050 MW_c.

The results validate the feasibility of utilizing nuclear heat for district cooling applications. The optimized design determines employing 11 nuclear plants, each with a capacity of 150 MW_t, eliminating the need for gas boilers. Through the optimization process, the largest capacities for heat storage and cold storage (20 000 MW_th) were chosen, reflecting the technoeconomic advantages of employing thermal energy storage to enhance the load-following capability and increase the capacity factor of the system.

This innovative approach effectively addresses two critical challenges in the air conditioning sector: high electricity consumption and the associated carbon emissions. Covering 92% of the cooling demand energy by absorption chillers driven by nuclear heat leads to considerable electricity and carbon emission saving of 69% compared to an electric-driven scenario. However, auxiliary compression chillers are still necessary for peak shaving, enhancing the load following and covering the low cooling demands periods when absorption chillers are inactive due to the heat transmission limits.

The economic competitiveness of the proposed system is confirmed, with a cost reduction of 34% for the 20 km heat transmission case compared to the electric-driven scenario. The sensitivity analyses demonstrate the influence of electricity price and heat transmission distance on the system's economics. As the distance decreases and electricity price increases, the proposed system becomes increasingly advantageous, and vice versa.

There is potential to modify and apply the proposed method to assess different types of energy sources for district cooling applications in future studies. Additionally, the method can be extended to evaluate systems with higher heat source temperatures that can drive double-effect absorption chillers. While this study focused on modeling the capacities of the supply units and heat transmission pumping as a whole, further optimization can be pursued to achieve more detailed sizing, placement of pumping stations, and configuration of the chillers. These additional steps can complement the overall optimization process and provide more comprehensive results for the system design and operation.

Nomenclature

A_{hex}: Heat transfer area of heat exchanger (m^2)
c: Flow velocity (m/s)
CG_{ac}^{i}: Hourly cooling power of absorption chillers (MWc)
CG_{cc}^{i}: Hourly cooling power of compression chillers (MWc)
CG_{cs}^{i}: Hourly charged/discharged cooling power by cold storage (MWc)
COP_{ac}, COP_{cc}: Average coefficient of performance of absorption and compression chillers
C_p: Specific heat capacity of water (W.s/kg.K)
Cp_{hex}: Thermal power capacity of heat exchanger (MWt)
Cp_{hs}: Thermal energy capacity of heat storage (MWth)
Cp_{ac}: Cooling capacity of absorption chillers (MWc)
Cp_{cc}: Cooling capacity of compression chillers (MWc)
Cp_{cs}: Cooling energy capacity of cold storage (MWch)
Cp_{gb}: Thermal capacity of gas boiler (MWt)
Cp_{nhp}: Thermal capacity of one nuclear plant (MWt)
Cp_{pump}: Electrical capacity of pumping station (MWe)
D, D_{out}: Inner diameter and outer diameter of heat transmission pipe (m)
EC_{ac}: Absorption chiller's auxiliary electrical power consumption per supplied cooling power (MWe/MWc) (%)
EC_{cc}: Compression chiller's auxiliary electrical power consumption per supplied cooling power (MWe/MWc) (%)
EC_{gb}: Gas boiler's auxiliary electrical power consumption per supplied thermal power (MWe/MWt) (%)
EC_{nhp}: Nuclear heat plant's auxiliary electrical power consumption per supplied thermal power (MWe/MWt) (%)
f: Friction factor
hi: Thermal conductivity of pipe insulation (W/m.K)
IC_{bht}: Initial capital cost of heat transmission system ($)
IC_{css}: Initial capital cost of cooling supply station ($)
IC_{hss}: Initial capital cost of the heat supply station ($)
IC_{hex}^{hss}, IC_{hex}^{css}: Initial capital cost of heat exchangers at the endpoints of the pipe (on heating station side and cooling station side) ($)
IC_{hs}: Initial capital cost of heat storage ($)
IC_{nhp}: Initial capital cost of the nuclear heat plants ($)
IC_{pipe}: Initial capital cost of pipes including insulation ($)

IC_{pump}: Initial capital cost of pressure-boosting pump ($)
IR: Annual interest rate (%)
L: The one-way pipeline length (m)
LMTD: The logarithmic mean temperature difference (K)
$\dot{m}^{i}_{bht}$: Hourly mass flow rate of water in transmission pipe (kg/s)
N: Number of hours in a year
N_{nhp}: Number of nuclear heat plants
OF: Objective function ($)
OM^{af}_{hss}: Annual fixed operation and maintenance (O&M) cost of heat supply station ($/yr)
OM^{av}_{hss}: Annual variable O&M cost of heat supply station ($/yr)
OMC_{hss}: Present value of total O&M cost of the heat supply station ($)
OMC_{bht}: Present value of total O&M cost of the heat transmission system ($)
OMC_{css}: Present value of total O&M cost of the cooling supply station ($)
P: Pumping power (MWe)
Q^{i}_{hs}: Hourly charged/discharged thermal power by heat storage (MWt)
Q^{HTL}: Heat transmission losses (MWt)
Q^{i}_{bht}: Hourly transported heat (MWt)
Q^{i}_{gb}: Hourly heat generation by gas boiler (MWt)
Q^{i}_{nhp}: Hourly heat generation by nuclear plants (MWt)
Re: Reynolds number
RR_{ac}: Ramp rate of absorption chilling (% of capacity)
R^{ch}_{hs}, R^{dch}_{hs}: Charging/discharging power rate of heat storage (% of capacity)
RC_{css}: Reconstruction cost of cooling supply station ($)
RC_{hss}: Reconstruction cost of heat supply station ($)
RC_{bht}: Reconstruction cost of bulk heat transmission system ($)
RR_{cc}: Ramp rate of compression chilling (% of capacity)
RR^{ch}_{cs}, RR^{dch}_{cs}: Charging/discharging power rate of the cold storage (% of capacity)
RR_{gb}: Ramp rate of gas boiler (% of capacity)
RR^{up}_{nhp}, RR^{down}_{nhp}: Increasing and decreasing ramp rates of nuclear units (% of capacity)
s: Pipe insulation thickness (mm)
SE^{i}_{hs}: Heat storage's stored thermal energy at the hour (i), (MWth)
SE^{i}_{cs}: Hourly cooling energy stored in cold storage (MWch)
SFC_{gb}: Specific fuel cost of gas boiler ($/MWth)
SFC_{nhp}: Specific fuel cost of nuclear plants ($/MWth)
Sg: Specific gravity of water
SOM^{f}_{hs}, SOM^{f}_{cs}: Specific fixed O&M cost of heat, cold storage ($/MWth/yr)
SOM^{f}_{ac}: Specific fixed O&M cost of absorption chiller ($/MWc/yr)
SOM^{v}_{ac}: Specific variable O&M cost of absorption chiller ($/MWch)
SOM^{f}_{cc}: Specific fixed O&M cost of compression chiller ($/MWc/yr)
SOM^{v}_{cc}: Specific variable O&M cost of compression chiller ($/MWch)
SOM^{f}_{gb}: Specific fixed O&M cost of gas boiler ($/MWt/yr)
SOM^{v}_{gb}: Specific variable O&M cost of gas boiler ($/MWth)
SOM^{f}_{nhp}: Specific fixed O&M cost of nuclear plants ($/MWt/yr)
SOM^{v}_{nhp}: Specific variable O&M cost of nuclear plants ($/MWth)
U: Heat transfer coefficient of heat exchanger ($W/m^2.K$
V^{s}_{cs}: Cold storage volume (m^3)
V_{ins}: Insulation volume (m^3)
Wt_{pipe}: Weight of pipe (kg)
ΔT_A: Temperature difference between the inlet hot water and outlet cold water of heat exchanger (K)
ΔT_B: Ttemperature difference between the outlet hot water and the inlet cold water of heat exchanger (K)
ΔT_{cs}: Cold storage supply/return difference temperature (K)
ΔT_{bht}: Difference between heat transmission supply and return temperatures (K)
ΔP: Pressure drop along the pipeline (kPa)
η_{ps}: Pump efficiency
η_{cs}: Efficiency of cold storage
ε: Roughness of the pipe (mm)
ν: Kinematic viscosity of water (m^2/s)
ρ: Density of water (kg/m^3).

Data Availability

Data is available on request. Contact us by the following email: abushama@fel.zcu.cz.

Conflicts of Interest

The authors declare that they have no known competing financial interests or personal relationships that could have appeared to influence the work reported in this paper.

Acknowledgments

This work was supported by the UWB university grant (SGS-2021-018) and the Czech Technological Agency grant (TK 03030109).

References

[1] IEA, *The Future of Cooling*, Opportunities for Energy-Efficient Air Conditioning. OECD/IEA, 2018.

[2] I. Andric and S. G. Al-Ghamdi, "Climate change implications for environmental performance of residential building energy use: the case of Qatar," *Energy Reports*, vol. 6, pp. 587–592, 2020.

[3] N. O. Bell, J. I. Bilbao, M. Kay, and A. B. Sproul, "Future climate scenarios and their impact on heating, ventilation and air-conditioning system design and performance for commercial buildings for 2050," *Renewable and Sustainable Energy Reviews*, vol. 162, p. 112363, 2022.

[4] H. A. Saleh Abushamah and R. Skoda, "Nuclear energy for district cooling systems – novel approach and its eco-environmental assessment method," *Energy*, vol. 250, p. 123824, 2022.

[5] A. Inayat and M. Raza, "District cooling system via renewable energy sources: a review," *Renewable and Sustainable Energy Reviews*, vol. 107, pp. 360–373, 2019.

[6] W. Gang, S. Wang, F. Xiao, and D. C. Gao, "District cooling systems: technology integration, system optimization, challenges and opportunities for applications," *Renewable and Sustainable Energy Reviews*, vol. 53, pp. 253–264, 2016.

[7] F. Sun, W. Xu, H. Chen, B. Hao, and X. Zhao, "Configuration optimization of solar-driven low temperature district heating and cooling system integrated with distributed water-lithium bromide absorption heat pumps," *Solar Energy*, vol. 253, pp. 401–413, 2023.

[8] M. Jannatabadi, H. R. Rahbari, and A. Arabkoohsar, "District cooling systems in Iranian energy matrix, a techno-economic analysis of a reliable solution for a serious challenge," *Energy*, vol. 214, p. 118914, 2021.

[9] H. Safa, "Heat recovery from nuclear power plants," *International Journal of Electrical Power & Energy Systems*, vol. 42, no. 1, pp. 553–559, 2012.

[10] M. Leurent, P. da Costa, M. Rämä, U. Persson, and F. Jasserand, "Cost-benefit analysis of district heating systems using heat from nuclear plants in seven European countries," *Energy*, vol. 149, pp. 454–472, 2018.

[11] K. C. Kavvadias and S. Quoilin, "Exploiting waste heat potential by long distance heat transmission: design considerations and techno-economic assessment," *Applied Energy*, vol. 216, pp. 452–465, 2018.

[12] P. Hirsch, K. Duzinkiewicz, M. Grochowski, and R. Piotrowski, "Two-phase optimizing approach to design assessments of long distance heat transportation for CHP systems," *Applied Energy*, vol. 182, pp. 164–176, 2016.

[13] P. C. Basu, "Site evaluation for nuclear power plants – the practices," *Nuclear Engineering and Design*, vol. 352, article 110140, 2019.

[14] R. Loisel, V. Alexeeva, A. Zucker, and D. Shropshire, "Load-following with nuclear power: market effects and welfare implications," *Progress in Nuclear Energy*, vol. 109, pp. 280–292, 2018.

[15] W. Zhang, X. Jin, and W. Hong, "The application and development of district cooling system in China: a review," *Journal of Building Engineering*, vol. 50, article 104166, 2022.

[16] R. Nikbakhti, X. Wang, A. K. Hussein, and A. Iranmanesh, "Absorption cooling systems – review of various techniques for energy performance enhancement," *Alexandria Engineering Journal*, vol. 59, no. 2, pp. 707–738, 2020.

[17] H. Subki, "Advances in small modular reactor technology developments," 2020, Accessed: Oct. 11, 2022, https://inis.iaea.org/search/search.aspx?orig_q=RN:51105613.

[18] R. Skoda, A. Fortova, D. Masata et al., "TEPLATOR: nuclear district heating solution," in *Proceedings of International Conference Nuclear Energy for New Europe*, pp. 221–228, Portorož, Slovenia, 2020.

[19] L. Zhang, Y. Wang, and X. Feng, "A framework for design and operation optimization for utilizing low-grade industrial waste heat in district heating and cooling," *Energies*, vol. 14, no. 8, p. 2190, 2021.

[20] C. Chang, X. Chen, Y. Wang, and X. Feng, "An efficient optimization algorithm for waste heat integration using a heat recovery loop between two plants," *Applied Thermal Engineering*, vol. 105, pp. 799–806, 2016.

[21] E. S. Menon, *Working Guide to Pump and Pumping Stations: Calculations and Simulations*, Gulf Professional Publishing, 2010.

[22] F. Ochs, A. Dahash, A. Tosatto, and M. Bianchi Janetti, "Techno-economic planning and construction of cost-effective large-scale hot water thermal energy storage for renewable district heating systems," *Renewable Energy*, vol. 150, pp. 1165–1177, 2020.

[23] "Technology data for energy storage," 2018, Accessed: Oct. 11, 2022, https://ens.dk/en/our-services/projections-and-models/technology-data/technology-data-energy-storage.

[24] M. Z. Stijepovic and P. Linke, "Optimal waste heat recovery and reuse in industrial zones," *Energy*, vol. 36, no. 7, pp. 4019–4031, 2011.

[25] D. Alghool, T. Elmekkawy, M. Haouari, and A. Elomri, "Data of the design of solar assisted district cooling systems," *Data in Brief*, vol. 30, article 105541, 2020.

[26] C. Lahoud, M. el Brouche, C. Lahoud, and M. Hmadi, "A review of single-effect solar absorption chillers and its perspective on Lebanese case," *Energy Reports*, vol. 7, pp. 12–22, 2021.

[27] "Absorption chillers and heat pumps," (accessed Nov. 07, 2022), http://worldenergy.co.kr/en/catalogue-2/.

[28] S. Lazarević, V. Čongradac, A. Andjelkovic, M. Kljajić, and Ž. Kanović, "District heating substation elements modeling for the development of the real-time model," *Thermal Science*, vol. 23, no. 3 Part B, pp. 2061–2070, 2019.

[29] Danish Energy Agency, *Technology Data for Generation of Electricity and District Heating*, Danish Energy Agency, 2020.

[30] "World energy absorption chiller absorption chiller & heater absorption heat pump," (accessed Oct. 11, 2022), https://www.worldenergyeurope.eu/products.html.

[31] "Electricity prices for non-household consumers in EU," (accessed Oct. 20, 2022), https://ec.europa.eu/eurostat/statistics-explained/index.php?title=Electricity_price_statistics#Electricity_prices_for_non-household_consumers.

[32] "Natural gas prices for non-household consumers in EU," (accessed Oct. 20, 2022), https://ec.europa.eu/eurostat/statistics-explained/index.php?title=Natural_gas_price_statistics#Natural_gas_prices_for_non-household_consumers.

[33] H. A. S. Abushamah, D. Masata, M. Mueller, and R. Skoda, "Economics of reusing spent nuclear fuel by Teplator for district heating applications," *International Journal of Energy Research*, vol. 46, no. 5, 2022.